

## Observation of signature inversion in the $\nu(h_{11/2}) \otimes \pi(h_{11/2})$ band of $^{122}\text{Cs}$

J. F. Smith,\* C. J. Chiara, D. B. Fossan, G. J. Lane,† J. F. Lewicki, J. M. Sears, and P. Vaska‡  
*Department of Physics and Astronomy, State University of New York at Stony Brook, Stony Brook, New York 11794-3800*  
 (Received 8 June 1998)

High-spin states have been studied in  $^{122}\text{Cs}$  using the  $^{94}\text{Mo}(^{31}\text{P},2pn)$  reaction. Two rotational bands have been observed to spins of 28 and 21  $\hbar$ . The most intensely populated band has been reassigned to have the  $\nu(h_{11/2}) \otimes \pi(h_{11/2})$  configuration. A low-spin signature inversion is observed in this band between 19 and 20  $\hbar$ , consistent with the neighboring odd-odd cesium isotopes. Spectroscopic properties are discussed, including signature inversion of bands in  $A \approx 120$  nuclei. [S0556-2813(98)03412-8]

PACS number(s): 21.10.Re, 23.20.Lv, 27.60.+j, 29.30.Kv

### I. INTRODUCTION

The odd-odd, neutron-deficient  $Z=55$  cesium isotopes are of particular interest because both the valence neutron and proton can occupy orbitals originating from the same high- $j$   $h_{11/2}$  intruder subshell, which can have competing shape-driving tendencies. The proton Fermi level lies near the low- $\Omega$   $h_{11/2}$  orbitals, which favor prolate nuclear shapes. In the  $A \approx 130$  cesium isotopes, the neutron Fermi level lies in the high- to mid- $\Omega$   $h_{11/2}$  orbitals, which favor oblate nuclear shapes. As the neutron number decreases towards  $A \approx 120$ , the cesium isotopes possess a variety of shapes depending on the Fermi level, the configuration of nucleons, and on the rotational frequency. In addition, as  $N$  decreases, the neutron Fermi level lowers into the low- $\Omega$   $h_{11/2}$  orbitals, while the proton Fermi level also lies in the low- $\Omega$   $h_{11/2}$  orbitals. With increasing spatial overlap, the possibility of a residual interaction between the valence proton and neutron arises. There is already some experimental evidence for  $pn$  interaction effects in this region [1,2].

The spectroscopy of odd-odd nuclei can be difficult because of the inevitably large number of low-lying excited states. These states are often connected by fragmented, low-energy decay paths. However, physics can often be easily extracted from the spectroscopy of these nuclei if they are sufficiently deformed for rotational bands to develop. The  $A \approx 120$  odd-odd cesium isotopes have well-developed quadrupole deformations with  $\beta_2 \approx 0.25$ . Certain rotational bands in these nuclei have recently been shown to exhibit a phenomenon known as *signature inversion* [3]. The signature quantum number,  $\alpha$ , is associated with the rotation of a deformed nucleus around a principal axis by  $180^\circ$ , and is defined as  $\alpha = I \bmod 2$ , where  $I$  is the angular momentum. By definition, the levels with favored signature  $\alpha_f$  lie lower in energy than those with unfavored signature. In

an odd-odd nucleus, the favored signature is given by  $\alpha_f = \frac{1}{2} [(-1)^{j_p - 1/2} + (-1)^{j_n - 1/2}]$ . Signature inversion describes the situation where, below an *inversion spin*, the levels with favored signature lie higher in energy than those with unfavored signature; that is, the signature splitting is inverted from what would be expected. The physics underlying signature inversion has been attributed to a variety of effects, most notably triaxiality [4] and the  $pn$  interaction [5]; at present, however, the theories cannot satisfactorily explain the experimental data. A low-spin signature inversion has been observed in bands based on the  $\nu(h_{11/2}) \otimes \pi(h_{11/2})$  configuration in  $^{118,120,124}\text{Cs}$  [1,6,7]. In these nuclei, the  $\nu(h_{11/2}) \otimes \pi(h_{11/2})$  band is populated with the largest fraction of the channel intensity. In  $^{122}\text{Cs}$ , the most intensely populated band had previously been assigned to have the  $\nu(g_{7/2}) \otimes \pi(h_{11/2})$  configuration [8]. Furthermore, the trend in signature splitting within the previously reported band suggests that a signature inversion may take place at higher spin than has so far been observed.

An experiment has been performed at the Nuclear Structure Laboratory at Stony Brook, in order to test the configuration assignment of Ref. [8] and to populate excited states up to and above the possible signature inversion. The reaction used in the present work was chosen to populate higher spin states in the  $^{122}\text{Cs}$  residue compared to that of Ref. [8] (semiclassical estimates suggest that  $\ell_{max} = 40\hbar$ , compared with  $\ell_{max} = 24\hbar$  in Ref. [8]). In this work, excited states in  $^{122}\text{Cs}$  have been observed up to  $28\hbar$ . The most intensely populated band has been reassigned to have the  $\nu(h_{11/2}) \otimes \pi(h_{11/2})$  configuration, primarily on the basis of quasiparticle alignments. A signature inversion is observed between spins 19 and 20  $\hbar$  (taking spin assignments from systematics) in agreement with the  $N$  dependence of the inversion spin in the  $\nu(h_{11/2}) \otimes \pi(h_{11/2})$  bands in neighboring odd-odd nuclei.

### II. EXPERIMENTAL DETAILS

High-spin states in  $^{122}\text{Cs}$  have been populated using the  $^{94}\text{Mo}(^{31}\text{P},2pn)$  reaction, with a beam energy of 127 MeV. The beam was provided by the Stony Brook FN-tandem/superconducting linac facility. The beam energy was chosen on the basis of an excitation study in which singles  $\gamma$ -ray data were collected for  $\sim 1$  h for several energies between 120 and 140 MeV, in order to maximize the cross section

\*Present address: Schuster Laboratory, The University of Manchester, Manchester, M13 9PL, United Kingdom.

†Present address: Department of Nuclear Physics, Research School of Physical Science and Engineering, Australian National University, Canberra, ACT 0200, Australia.

‡Present address: UGM Laboratory, Inc, 3611 Market Street, Philadelphia, PA 19104.

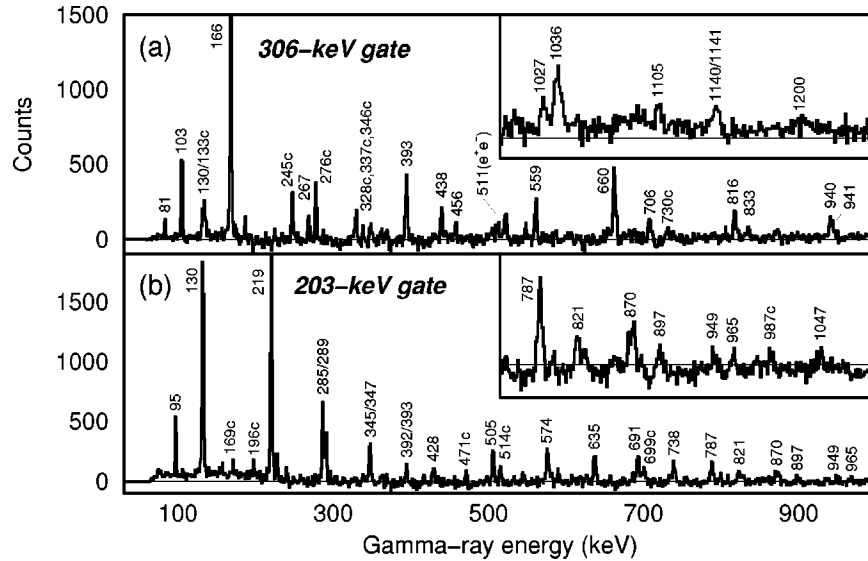


FIG. 1. Representative  $\gamma$ -ray spectra, generated by single gates on the  $\gamma$ - $\gamma$  matrix: (a) shows a gate on the 306-keV ( $13^+ \rightarrow 12^+$ ) transition in Band 1 and (b) shows a gate on the 203-keV ( $8^- \rightarrow 7^-$ ) transition in Band 2. The insets show the high-energy parts of the respective spectra shown on expanded scales. The numbers marking the peaks are transition energies given to the nearest keV. Transitions labeled with the letter *c* indicate known contaminants.

for  $^{122}\text{Cs}$ . The target consisted of a self-supporting  $900 \mu\text{g}/\text{cm}^2$   $^{94}\text{Mo}$  foil enriched to  $93.9(\pm 0.1)\%$ .

Data were collected using the Stony Brook array of six high-purity germanium detectors, each with an efficiency of approximately 25% of that of a  $3 \times 3$  in NaI(Tl) detector. After approximately 3 days,  $20 \times 10^6$   $\gamma$ - $\gamma$  coincidences were recorded onto magnetic tape. In the off-line analysis, the data were sorted into a two-dimensional  $\gamma$ - $\gamma$  matrix with  $\gamma$ -ray energy on each axis. One-dimensional spectra were projected from the matrix using the RADWARE code ESCL8R [9]. By gating on known transitions, over 10 evaporation residues were observed in the data. The most intensely populated evaporation residues were  $^{122}\text{Ba}$  ( $p2n$  evaporation) and  $^{121}\text{Cs}$  ( $2p2n$ ), which constituted  $\sim 33\%$  and  $\sim 26\%$  of the data, respectively. The  $^{122}\text{Cs}$  residue was the third most strongly populated, and constituted  $\sim 13\%$  of the data. Representative spectra gated on known transitions in  $^{122}\text{Cs}$  are shown in Fig. 1.

### III. RESULTS

#### A. The level scheme of $^{122}\text{Cs}$

By gating on the  $\gamma$ - $\gamma$  matrix, two bands, Band 1 and Band 2 shown in Fig. 2, were deduced. No transitions were observed connecting the bands to each other. Only two transitions (103 and 130 keV) were observed to decay from Band 1 and no transitions were observed from Band 2. The lack of observation of transitions below either of the bands is presumably because the bands exist at excitation energies above many lower spin states, as is often the case for odd-odd nuclei, such that the decay proceeds via fragmented parallel paths with low-energy, low-intensity transitions. Band 1 was populated with approximately five times the intensity of Band 2. Configuration assignments have been made primarily on the basis of the observed aligned angular momenta, and the reasons for the assignments are discussed in Sec. IV. Band 1 has been assigned to have the  $\nu(h_{11/2}) \otimes \pi(h_{11/2})$

configuration. In this band, two  $\Delta I=2$  sequences have been observed, ranging from spins 11 and 12  $\hbar$  to 27 and 28  $\hbar$ , respectively. Below about 19  $\hbar$ , the two sequences are connected by  $\Delta I=1$  transitions. The signature splitting within the band is not constant, but varies with spin. Indeed, the signature splitting changes sign at a spin of about 20  $\hbar$ ; this signature inversion is of particular interest and is discussed later in more detail. Band 2 has been assigned to have the  $\nu(h_{11/2}) \otimes \pi(g_{7/2})$  configuration. This band also consists of two  $\Delta I=2$  sequences, ranging from spins 5 and 6  $\hbar$  to 21 and 20  $\hbar$ , respectively. Below spin 16  $\hbar$ , the two sequences are connected by  $\Delta I=1$  transitions. The signature splitting is nearly zero over the observed range of spins.

The bands are not connected to any states of known spin and parity. The spins of the bands have therefore been tentatively assigned, primarily on the basis of systematics. In Ref. [3], Liu *et al.* have systematically studied the  $\nu(h_{11/2}) \otimes \pi(h_{11/2})$  bands of  $^{120-130}\text{Cs}$ . They have used excitation-energy systematics to assign spins to the bands; in the present work the spins of band 1 have been made consistent with the level schemes of Ref. [3]. It is possible that these spin assignments are 2  $\hbar$  too high, dependent upon the spin of the band-head in  $^{130}\text{Cs}$  (see Ref. [3] and also Ref. [10]). It should be remembered that the use of systematics can be unreliable because dynamic effects, such as band crossings, can cause perturbations. However, in this case the smoothly varying excitation energies as a function of spin, shown in Ref. [3], would seemingly rule out such effects. The spin of the band head of band 2 has been made consistent with analogous bands in the neighboring isotopes  $^{118,120}\text{Cs}$  [1,6]. The spins of the states above the band head have been assigned on the basis of the directional-correlation analysis of Ref. [8]. The low intensity of the  $^{122}\text{Cs}$  evaporation channel in the present experiment, and the larger number of contaminants in the spectra due to the high fragmentation of the evaporation-residue cross section, meant that it was not possible to improve the accuracy of the previously measured

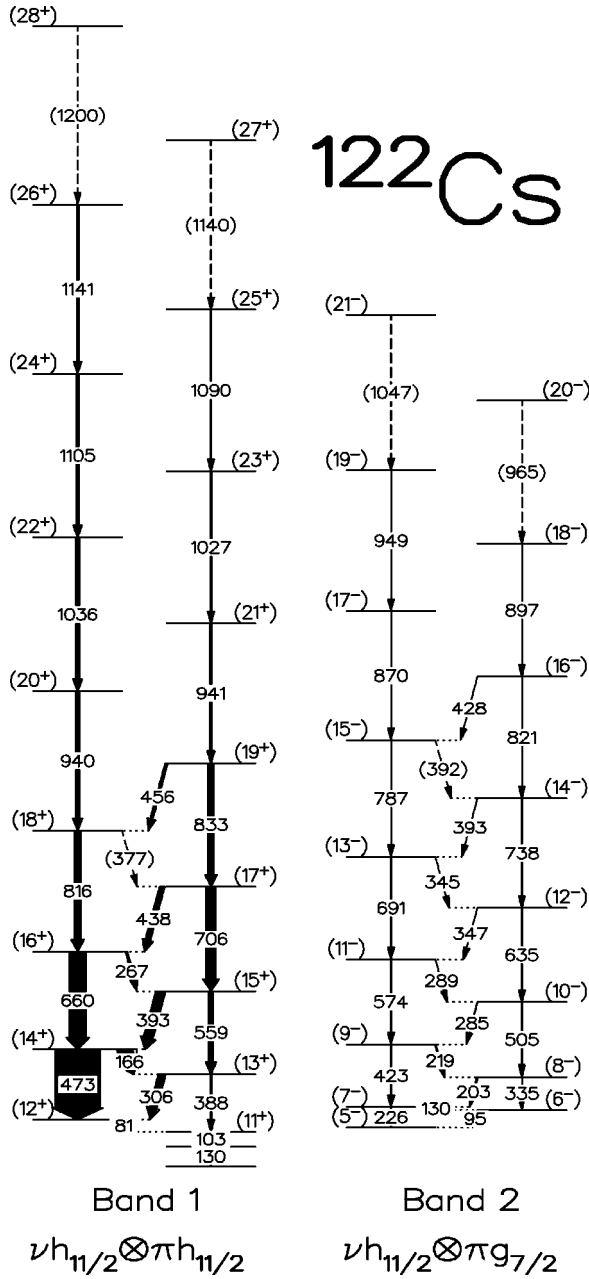


FIG. 2. The level structure of the bands in  $^{122}\text{Cs}$  observed in this work. The spin and parity assignments are discussed in the text. The widths of the arrows are proportional to the measured  $\gamma$ -ray intensities. If the  $\gamma$ -ray energy is given in parentheses, the transition is tentative. The errors on the energies range from 0.1 to 0.5 keV, and the errors on the intensities range from 10 to 30 %, with the doublets and weak transitions having the largest associated errors.

directional-correlation ratios. The newly observed  $\gamma$ -ray transitions which are all extensions of the  $\Delta I=2$  sequences observed in each band, and which were not observed in Ref. [8], have been assumed to have stretched electric-quadrupole character.

### B. Comparison with previous work

There are some discrepancies between this work and that of Xu *et al.* [8], which will be briefly addressed here. In Ref. [8], band 1 was observed up to a spin of about  $20 \hbar$  (quoting spin assignments from the present work) at which point the

TABLE I. Calculated deformations, predicted by TRS calculations, and quasiparticle alignment frequencies for (a) the  $\nu(h_{11/2}) \otimes \pi(h_{11/2})$  configuration and (b) the  $\nu(h_{11/2}) \otimes \pi(g_{7/2})$  configuration. The labels *ef*, *fg*, and *ab* refer to the first and second pairs of  $h_{11/2}$  orbitals, and the first pair of  $g_{7/2}$  orbitals, respectively. The letter *B* in parentheses indicates that the alignment will be blocked, for the given configuration.

(a) $\nu(h_{11/2}) \otimes \pi(h_{11/2})$ : $\beta_2=0.248$ $\gamma=5^\circ$ $\beta_4=0.008$			
$\omega$ (MeV/ $\hbar$ )			
	<i>ef</i>	<i>fg</i>	<i>ab</i>
Protons	0.36 ( <i>B</i> )	0.70	$\sim 0.7$
Neutrons	0.37 ( <i>B</i> )	0.50	$\sim 0.65$

(b) $\nu(h_{11/2}) \otimes \pi(g_{7/2})$ : $\beta_2=0.230$ $\gamma=-1^\circ$ $\beta_4=0.001$			
$\omega$ (MeV/ $\hbar$ )			
	<i>ef</i>	<i>fg</i>	<i>ab</i>
Protons	0.41	0.73	$> 0.7$
Neutrons	0.34 ( <i>B</i> )	0.45	$> 0.7$

rotational alignment of a pair of  $h_{11/2}$  neutrons was suggested, causing an increase in signature splitting and the subsequent loss of observation of the unfavored signature sequence. Several transitions were observed above the alignment in the favored signature sequence. Primarily on this basis, band 1 was assigned to be based on the  $\nu(g_{7/2}) \otimes \pi(h_{11/2})$  configuration. Band 2 was assigned to be based on the  $\nu(h_{11/2}) \otimes \pi(g_{7/2})$  configuration. In the present work, the two signature partners of Band 1 are observed to spins 28 and 27  $\hbar$ , and the alignment reported in Ref. [8] is not observed. For reasons discussed below, Band 1 has been reassigned to have the  $\nu(h_{11/2}) \otimes \pi(h_{11/2})$  configuration. Band 2 most likely has the  $\nu(h_{11/2}) \otimes \pi(g_{7/2})$  configuration, in agreement with Ref. [8]. It should also be pointed out that in Ref. [8] a 488-keV transition was observed linking the bands that established their relative excitation energies. However, the existence of the 488-keV transition could not be confirmed in the present work.

## IV. DISCUSSION

### A. Quasiparticle alignments

The configurations of the bands can be investigated by comparing their quasiparticle alignments to the predictions of the cranked shell model. Total-Routhian surface (TRS) calculations [11,12] have been used to predict the deformation parameters for various configurations of the valence neutron and proton. These deformation parameters have subsequently been used as input into cranked Woods-Saxon calculations in order to extract quasiparticle alignment frequencies for the lowest two pairs of  $h_{11/2}$  neutrons and protons, and also of  $g_{7/2}$  neutrons and protons. The results of the calculations are summarized in Table I.

The experimental aligned angular momenta of the bands are shown as a function of rotational frequency in Fig. 3. For all of the data points, a reference configuration, with Harris parameters [13] of  $\mathcal{J}_0=17.0 \text{ MeV}^{-1} \hbar^2$  and  $\mathcal{J}_1=25.8 \text{ MeV}^{-3} \hbar^4$ , has been subtracted. The large initial alignment of 9  $\hbar$  in band 1 is indicative of a configuration

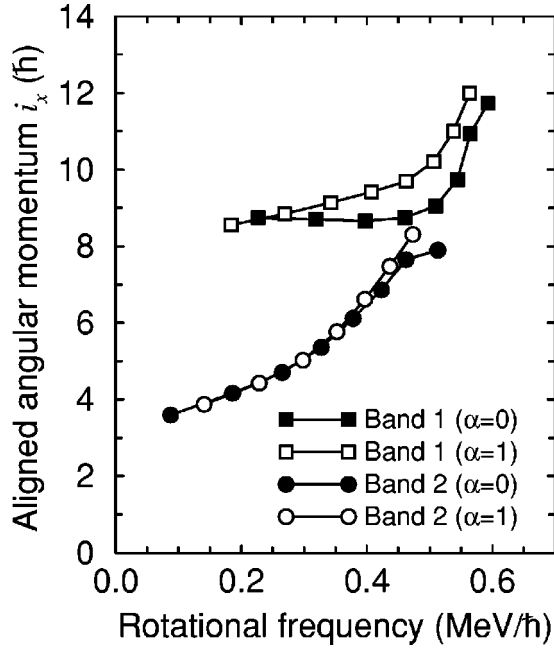


FIG. 3. Aligned angular momenta  $i_x$  plotted as a function of rotational frequency for the bands in  $^{122}\text{Cs}$ . For all data points a reference configuration with Harris parameters of  $\mathcal{J}_0 = 17.0 \text{ MeV}^{-1} \hbar^2$  and  $\mathcal{J}_1 = 25.8 \text{ MeV}^{-3} \hbar^4$ , has been subtracted. The  $\Delta I=2$  sequences with opposite signature quantum number  $\alpha$  are shown by closed ( $\alpha=0$ ) and open ( $\alpha=1$ ) symbols.

involving high- $j$  quasiparticles, and is consistent with the band being based on the  $\nu(h_{11/2}) \otimes \pi(h_{11/2})$  configuration. Table I reveals that, at the deformation calculated for the  $\nu(h_{11/2}) \otimes \pi(h_{11/2})$  configuration, the rotational alignment of the first pairs of  $h_{11/2}$  neutrons and protons (known as the  $ef$  alignments) are predicted to occur at very nearly the same frequencies of 0.36 and 0.37 MeV/ $\hbar$ , respectively. In Band 1, the first alignment is observed at  $\sim 0.5$  MeV/ $\hbar$ . This observation is consistent with Band 1 having the  $\nu(h_{11/2}) \otimes \pi(h_{11/2})$  configuration for which the alignments of the first pairs ( $ef$ ) of both neutrons and protons would be blocked, but where the alignment of the second pair of  $h_{11/2}$  neutrons ( $fg$ ) would be expected at 0.50 MeV/ $\hbar$ . The initial alignment of Band 2 is lower than that of Band 1, suggesting that the underlying configuration involves lower- $j$  nucleons. Furthermore, Band 2 does not have a sharp upbend like Band 1, but has a gradual upbend. This is consistent with the alignment of  $h_{11/2}$  protons at  $\sim 0.4$  MeV/ $\hbar$ , which would be expected if the band is based on the  $\nu(h_{11/2}) \otimes \pi(g_{7/2})$  configuration. The alignments of pairs of neutrons or protons from the  $g_{7/2}$  subshell ( $ab$  alignment) occur at rotational frequencies above those observed in this experiment.

### B. Transition strength ratios

To further investigate the underlying structure of the bands, the ratios of the reduced transition probabilities  $B(M1)/B(E2)$  have been studied. The experimentally extracted values have been compared to semiclassical estimates made using the Dönau and Frauendorf formalism [14,15]. Though inherent ambiguities, such as the alignment  $i_x$  of the quasiparticles and the size of the rotational gyromagnetic ratio  $g_R$ , prevent the deduction of precise  $B(M1)/B(E2)$

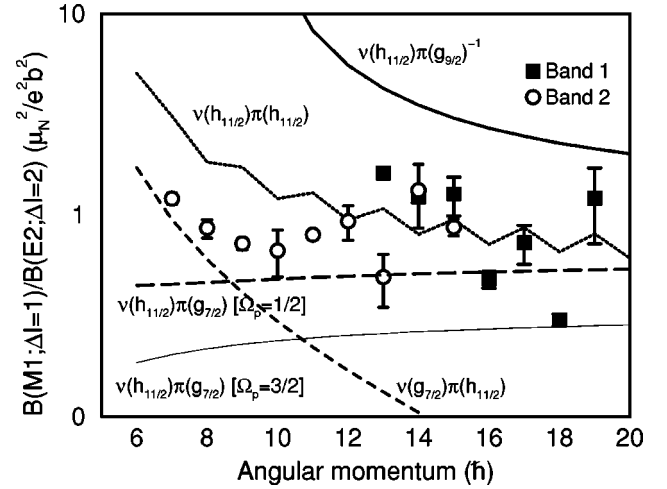


FIG. 4. The measured  $B(M1; \Delta I=1)/B(E2; \Delta I=2)$  ratios, compared to those predicted using the semiclassical formalism of Dönau and Frauendorf. The lines represent the calculated values. A signature-dependent term was included in the calculations, which introduces the staggering in the calculations for the  $\nu(h_{11/2}) \otimes \pi(h_{11/2})$  configuration.

ratios, their values can provide additional evidence for, or against, a proposed configuration. In this work  $B(M1)/B(E2)$  ratios have served to eliminate a possible configuration for Band 2 involving a  $g_{9/2}$  proton hole. The experimental  $B(M1)/B(E2)$  ratios have been extracted from the data using the relation

$$\frac{B(M1; \Delta I=1)}{B(E2; \Delta I=2)} = \frac{0.697}{(1 + \delta^2)} \frac{I_\gamma(M1)}{I_\gamma(E2)} \frac{E_\gamma^5(E2)}{E_\gamma^3(M1)}, \quad (1)$$

where  $I_\gamma$  represents  $\gamma$ -ray intensity and  $E_\gamma$  is the  $\gamma$ -ray energy in units of MeV. The mixing ratio  $\delta$  has been assumed to be zero, meaning that the experimental values plotted in Fig. 4 are upper limits. Also shown in the figure are the values calculated using the Dönau and Frauendorf formalism for various configurations. The parameters used in the calculations are summarized in Table II. In the calculations, the quadrupole moments used were deduced from TRS calculations, and the standard approximation of  $g_R = 0.7 Z/A$  was used. The signature splitting, which was included in the calculations, was estimated from the level scheme. The large error bars on some of the data points are a consequence of the reaction that was chosen to populate high-spin states; the large number of nuclei produced ( $>10$ ) meant that there were many degenerate transitions in the matrix, and often it

TABLE II. Summary of parameters used to calculate the Dönau and Frauendorf estimates of  $B(M1)/B(E2)$  ratios.

	Nilsson orbital	$K$	$i$	$g_K$
$\pi(h_{11/2})$	[550]1/2 <sup>-</sup>	1/2	5.0	1.214
$\pi(g_{7/2})$	[422]3/2 <sup>+</sup>	3/2	3.0	0.739
$\pi(g_{7/2})$	[420]1/2 <sup>+</sup>	1/2	3.5	0.739
$\pi(g_{9/2})^{-1}$	[404]9/2 <sup>+</sup>	9/2	0.5	1.261
$\nu(h_{11/2})$	[523]7/2 <sup>-</sup>	7/2	4.5	-0.209
$\nu(g_{7/2})$	[413]5/2 <sup>+</sup>	5/2	3.0	0.255

was not possible to produce uncontaminated spectra from gates directly above the state of interest. The values measured for Band 1 are reasonably consistent with the calculations for the  $\nu(h_{11/2}) \otimes \pi(h_{11/2})$  configuration. Furthermore, the ratios for the states that (presumably) have odd spin are larger than those with even spin, in agreement with the calculations and with the values measured in Ref. [8]. For Band 2, the ratios are in moderate agreement with the calculations for the  $\nu(h_{11/2}) \otimes \pi(g_{7/2})$  configuration. If  $|\delta| > 0$  for Band 2, this would bring the experimental data points closer to those calculated. The lack of signature splitting in this band suggests that an alternative possible configuration for this band would be  $\nu(h_{11/2}) \otimes \pi(g_{9/2})^{-1}$ . Bands with this configuration have been observed in  $^{118,120}\text{Cs}$  [1,16]. However, the values calculated for this configuration are clearly not in agreement with the experimental data points for Band 2.

Another possible configuration for Band 2 is  $\nu(g_{7/2}) \otimes \pi(h_{11/2})$ . This may be expected *a priori* because this is the configuration of the second most strongly populated band in both  $^{120}\text{Cs}$  [1] and  $^{118}\text{Cs}$  [16]. The aligned-angular momentum and blocking arguments cannot definitively distinguish between the two configurations, because the first  $h_{11/2}$  neutron and  $h_{11/2}$  proton alignments, given in Table I, occur at very nearly the same rotational frequency. The extracted  $B(M1)/B(E2)$  ratios, however, support the proposed  $\nu(h_{11/2}) \otimes \pi(g_{7/2})$  assignment, since the calculations for the  $\nu(h_{11/2}) \otimes \pi(g_{7/2})$  configuration are in better agreement with the experimental data than those for the  $\nu(g_{7/2}) \otimes \pi(h_{11/2})$  configuration. Furthermore, cranked shell model calculations suggest that the  $\nu(g_{7/2}) \otimes \pi(h_{11/2})$  band will possess a degree of signature splitting [8], whereas Band 2 has no signature splitting. Despite these arguments it must be stated that the configuration of Band 2 is not as well defined by this work as that of Band 1.

### C. Signature inversion in band 1

Inspection of Fig. 2 reveals that below about spin  $\sim 19 \hbar$  the levels with unfavored signature lie lower in energy than those with favored signature. This is illustrated in Fig. 5(a) where the quantity  $[E(I) - E(I-1)]/I$  is plotted against  $I$  for band 1, where  $E(I)$  is the energy of the level with spin  $I$ . The signature inversion in this band occurs between spins 19 and 20  $\hbar$ . Figure 5(b) shows the approximate inversion spins in the  $\nu(h_{11/2}) \otimes \pi(h_{11/2})$  bands in iodine ( $Z=53$ ), cesium ( $Z=55$ ) and lanthanum ( $Z=57$ ) isotopes. The inversion spin in  $^{122}\text{Cs}$  is clearly in systematic agreement with the bands in the neighboring nuclei.

At present, the physics underlying signature inversion is not understood. A variety of calculations have been made for the signature inversions in the  $\nu(i_{13/2}) \otimes \pi(h_{11/2})$  bands in  $A \approx 160$  nuclei. The first calculations suggested that a triaxial nuclear shape was solely responsible for the inversions [4], but later the inversions were reproduced using a  $pn$  interaction in particle-rotor model calculations assuming an axially symmetric shape [5]. Recent results for  $\nu(i_{13/2}) \otimes \pi(h_{9/2})$  bands in some  $A \approx 160-170$  nuclei have shown that triaxiality and Coriolis effects [19] alone are not sufficient to explain the data and a residual  $pn$  interaction must be included in calculations [20]. In a completely different approach, projected shell model calculations suggest that the inversions

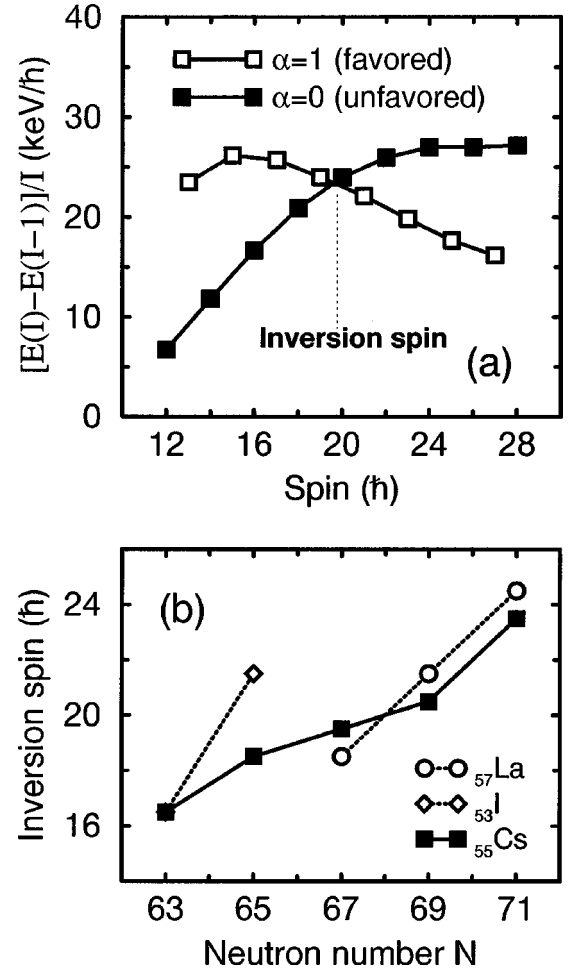


FIG. 5. (a) shows the quantity  $[E(I) - E(I-1)]/I$  plotted against spin, for the  $\pi(h_{11/2}) \otimes \nu(h_{11/2})$  band (Band 1). (b) shows the inversion spin plotted as a function of neutron number for the odd-odd iodine ( $Z=53$ ), cesium ( $Z=55$ ), and lanthanum ( $Z=57$ ) isotopes with  $63 \leq N \leq 71$ . The data are taken from the following references:  $^{116}\text{I}$  [17],  $^{118}\text{I}$  [18],  $^{118}\text{Cs}$  [6],  $^{120}\text{Cs}$  [1], and  $^{124,126}\text{Cs}$ ,  $^{124,126,128}\text{La}$  [7].

may be due to a band crossing [21,22]. At present the only calculations for the  $A = 120$  region have used the particle-rotor model but have found it necessary to invoke large triaxial deformations of  $\gamma \approx 25^\circ$  [23]. The TRS calculations (Table I) would suggest that such large triaxiality does not apply to  $^{122}\text{Cs}$  or to the lighter  $^{118,120}\text{Cs}$  isotopes [1,6]. The reassignment of the configuration of Band 1 in this work reinforces the point that signature inversion in the  $A \approx 120$  region is only observed in  $\nu(h_{11/2}) \otimes \pi(h_{11/2})$  bands. The reason why signature inversion is only observed in these bands and not in bands based on other configurations is also not understood. Calculations that can reproduce the systematic trends across isotopic and isotonic chains are needed in order to establish the relative importance of Coriolis effects, triaxiality, and a residual  $pn$  interaction.

### V. SUMMARY

In summary, high-spin states have been studied in  $^{122}\text{Cs}$  using the Stony Brook array. Two rotational bands have been observed up to spins of 28  $\hbar$  and 21  $\hbar$ , respectively. The

most intensely populated band has been reassigned to have the  $\nu(h_{11/2}) \otimes \pi(h_{11/2})$  configuration, primarily on the basis of the observed quasiparticle alignments. This band undergoes a signature inversion at  $19 \hbar$ , in systematic agreement with the neighboring odd-odd nuclei. An important conclusion from the present work is the confirmation that a low-spin signature inversion in the  $A \approx 120$  region has only been observed to occur in bands based on the  $\nu(h_{11/2}) \otimes \pi(h_{11/2})$  configuration. TRS calculations suggest that the  $\nu(h_{11/2}) \otimes \pi(h_{11/2})$  band in  $^{122}\text{Cs}$  has only modest triaxial deformation, suggesting that triaxiality is not the underlying cause of

the inversion. This work highlights the absence of any satisfactory calculations for the  $A \approx 120$  nuclei and reiterates the need for calculations to be performed to explain the low-spin signature inversions in nuclei of this mass region.

#### ACKNOWLEDGMENTS

This work was supported by the National Science Foundation. The authors would like to thank Andrzej Lipski for target preparation. The TRS codes were provided by R. Wyss and W. Nazarewicz.

- 
- [1] B. Cederwall *et al.*, Nucl. Phys. **A542**, 454 (1992).
  - [2] F. Lidén *et al.*, Nucl. Phys. **A550**, 365 (1992).
  - [3] Yunzho Liu, Jingbin Lu, Yingjun Ma, Shangui Zhou, and Hua Zheng, Phys. Rev. C **54**, 719 (1996).
  - [4] R. Bengtsson, H. Frisk, F. R. May, and J. A. Pinston, Nucl. Phys. **A415**, 189 (1984); R. Bengtsson and H. Frisk, *ibid.* **A437**, 263 (1985); J. A. Pinston, S. Andre, D. Barneoud, C. Foin, J. Genevey, and H. Frisk, Phys. Lett. **137B**, 47 (1984).
  - [5] P. B. Semmes and I. Ragnarsson, in *Proceedings of the Conference on High Spin Physics and Gamma Soft Nuclei*, edited by J. X. Saladin, R. A. Sorenson, and C. M. Vincent (World Scientific, Singapore, 1991), p. 500.
  - [6] J. F. Smith *et al.*, Phys. Lett. B **406**, 7 (1997).
  - [7] T. Komatsubara *et al.*, Nucl. Phys. **A557**, 419c (1993).
  - [8] N. Xu, Y. Liang, R. Ma, E. S. Paul, D. B. Fossan, and H. M. Latvakoski, Phys. Rev. C **41**, 2681 (1990).
  - [9] D. C. Radford, Nucl. Instrum. Methods Phys. Res. A **361**, 297 (1995); D. C. Radford, *ibid.* **361**, 306 (1995).
  - [10] Yunzho Liu, Jingbin Lu, Yingjun Ma, Guangyi Zhao, Hua Zheng, and Shangui Zhou, Phys. Rev. C **58**, 1849 (1998).
  - [11] R. Wyss, J. Nyberg, A. Johnson, R. Bengtsson, and W. Nazarewicz, Phys. Lett. B **215**, 211 (1989).
  - [12] W. Nazarewicz, G. A. Leander, and A. Johnson, Nucl. Phys. **A503**, 285 (1989).
  - [13] S. M. Harris, Phys. Rev. **138**, B509 (1965).
  - [14] F. Dönau and S. Frauendorf, in *Proceedings of the Conference on High Angular Momentum Properties of Nuclei*, Oak Ridge, 1982, edited by N. R. Johnson (Harwood Academic, New York, 1983), p. 143; F. Dönau, Nucl. Phys. **A471**, 469 (1987).
  - [15] S. Törmanen *et al.*, Nucl. Phys. **A572**, 417 (1994).
  - [16] J. F. Smith *et al.* (unpublished).
  - [17] E. S. Paul, D. B. Fossan, K. Hauschild, I. M. Hibbert, H. Schnare, J. M. Sears, I. Thorslund, R. Wadsworth, A. N. Wilson, and J. N. Wilson, J. Phys. G **21**, 995 (1995).
  - [18] E. S. Paul, D. B. Fossan, K. Hauschild, I. M. Hibbert, H. Schnare, J. M. Sears, I. Thorslund, R. Wadsworth, A. N. Wilson, and J. N. Wilson, J. Phys. G **22**, 653 (1996).
  - [19] I. Hammamoto, Phys. Lett. B **235**, 221 (1990).
  - [20] R. A. Bark *et al.*, Phys. Lett. B **406**, 193 (1997).
  - [21] K. Hara and Y. Sun, Nucl. Phys. **A531**, 221 (1991).
  - [22] J. Y. Zhang and Y. Sun (private communication).
  - [23] N. Tajima, Nucl. Phys. **A572**, 365 (1995).